Application of ICA and contourlet transform in image watermarking

Jia Mo
University of Electronic Science and Technology of China
School of Computer Science and Engineering
Chengdu 611731
East China Jiaotong University
Nanchang 330013
China
moorechia@gmail.com

Zhaofeng Ma,Yixian Yang, Xinxin Niu
Beijing University of Posts and Telecommunications
Information Security Center
Beijing 100876
China

Shuhua Xu
Shaoxing University
Mathematical Information College,
Shaoxing, Zhejiang 312000
China

Abstract: Based on independent component analysis (ICA) and contourlet, this paper designs an important robust watermarking scheme that mainly consists of watermark embedding and extracting. The embedding is done by mixing the host image signals and the watermarking signals through , the linear system of ICA model. The extracting is achieved by estimating the demixing matrix and the watermarking signals through ICA model. The scheme takes advantage of human visual system (HVS) to conduct a self-adaptive computation of the scaling factor matrix. The experiment uses PSNR and NCC to evaluate its imperceptibility and robustness, finding that the scheme functions well in resisting frequent attacks including filter, noise, cropping and mirror.

Key–Words: Image processing; watermarking; ICA; contourlet transform; HVS; robustness

1 Introduction

Along with the rapid development of multimedia and networking technology, digital works has been increasingly widespread, facilitating the publishing, distributing and changing of information. Digital watermark technology as a significant method for copyright protection has become a study focus in recent years.

According to the embedding route, watermarking can mainly be divided into the spatial domain and the transform domain [1]. The spatial domain is to embed the watermark by changing the pixel values of the primitive image. LSB (Last Significant Bit) and patchwork are two examples of this kind. Comparatively, this sort of algorithm is simple and real-time but not so good as the transform one in terms of the robustness. For the transform domain, the digital carrier is firstly conducted an orthogonal transformation to select some frequency bands and modify the coefficient of the bands in accordance with a certain rule. Then the inversion of orthogonal transformation is performed to get the watermark embedded image. The transform domain makes the best of human senses and thus enjoys good imperceptibility, robustness and compatibility with compression standards. The transform domain is typically represented by DWT [2], DCT [3] and DFT [4]. Recently, contourlet [5] as an emerging transform has been widely applied in image analysis and processing but not in watermark embedding. M.Jayalakshmi etc [6] proposed a blind watermark embedding algorithm in contourlet domain in 2006, followed by studies combining contourlet and watermarking [7][8].

As a major method in signal processing and data analysis, ICA model is applied by T.V Nguyen etc. in watermark analysis and processing because the model shared great similarity with watermarking [9]. Reference [10] used ICA to achieve a robust watermarking in DCT domain. Reference [11] employed ridgelet transform to enhance the image edge and reducing noises, projecting the image into a basis with its components as statistically independent as possible through ICA. Reference [12] put forward an approach to embed watermark in multimedia products by combining redundant discrete wavelet transform (RDWT) and independent component analysis. In this approach, the primitive image is decomposed by RDWT and watermark is embedded into LL subband frequency by mixing model of ICA. Reference [13] designed a blind watermark in DCT domain of colored image. Compared with wavelet and ridgelet transform, contourlet is characterized by its better image capturing ability. In this view, the paper designs a self-adaptive gray watermark scheme based on ICA and contourlet transform.

This paper is designed according to the following parts: Section 2 and 3 respectively introduce contourlet transform and ICA; Section 4 elaborates the watermarking scheme; Section 5 deals with the computation of the scaling factor and Section 6 the results with the conclusion in the end.

2 Contourlet Transform

Contourlet transform is a new two dimensional image presenting method characterized by its multiresolution, local positioning, multi-directionality, neighbor boundary sampling and anisotropy. The primary function, distributed in a variety of scales and directions, can effectively capture the edge contour of images with fewer coefficients.

The fundamental principle of contourlet transform is firstly to use a wavelet-like multiscale decomposition to capture singular values of the edge and then assemble the neighboring singular values into the contour segment. Laplacian pyramid (LP) is used to perform a multiresolution decomposition over the image to capture the singular points shown in Fig. 1.

Directional filter bank (DFB) is adopted to link these point discontinuities into linear structures. Based on the understanding, contourlet transform is considered as a dual filter structure named as pyramidal directional filter bank (PDFB) in Fig.2. In addition to the integrated attributes of LP and DBF, the transform also enjoys its unique features that can be explained below [5].

(1) PDFB offers the tense frame of which the boundary frame is 1 when LP and DBF are done by orthogonal filters.

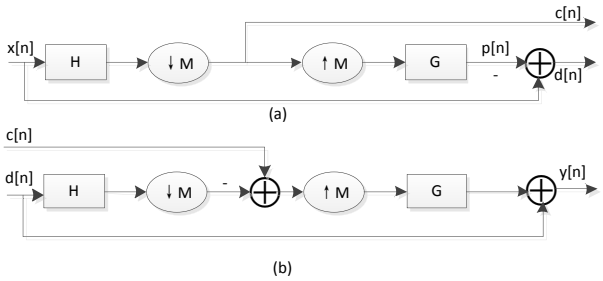

Figure 1: (a)LP decomposition (b)LP reconstruction

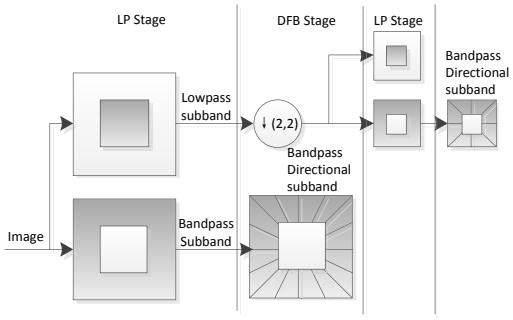

Figure 2: Contourlet filter bank structure

(2) PDFB enables to restructure the primitive image when LP and DBF are done by complete restructuring filters.

(3) The computing complexity of N- pixel image by PDFB is $O(N)$ when using finite impulse response (FIR) filter.

(4) The supporting set for PDFB-base image is 2^{j+l_j-2} in length and 2^j in width when the highpass subband obtained by decomposing the j level of LP is input into DFB, the l_j binary tree.

(5) The redundancy for PDFB comes from LP and its upper limit is 4/3.

Contourlet transform provides a flexible image multiresolution presentation. Compared with wavelet, contourlet represents richer directions and shapes while 2D wavelet transform can only capture information in horizontal, vertical and diagonal directions. Besides, contourlet transform performs better in depicting the geometrical structure of images.After contourlet transform, the low frequency subimages gather most energy and consequently they suffer little impact caused by regular image processing. This paper embeds the watermark into the low frequency subimages. The host image Lena after two-level contourlet transforms is illustrated in Fig.3.

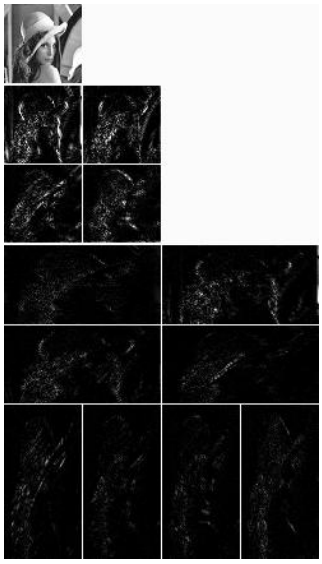

Figure 3: Contourlet transform of Lena image

3 ICA

Independent component analysis (ICA) [12] is a technology separating independent source signals from the linearly mixing observed signals based on statistical independence. It can be applied in blind source separation, feature extraction, image denoising and digital watermarking and so on. The fundamental principle is here explained: the statistically independent source signals s, $s = (s_1, s_2, ..., s_n)^T$, are mixed through the linear system A. to get the observed signals x, $x = (x_1, x_2, ..., x_n)^T$. That is, $x = As$ in which s and A are unknown. ICA aims to estimate the value of s and A by the observed signal x,that is, $y = Bx$, in which BBA^{-1},as is shown in figure 4.

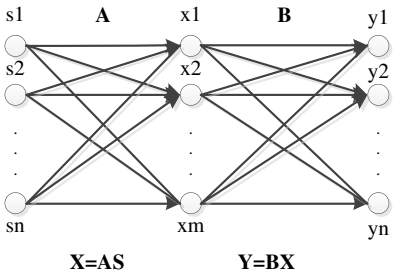

Figure 4: ICA model

ICA aims at finding a set of linear non-orthogonal coordinate to obtain a set of statistically independent variables by operating the linear non-orthogonal transformation over the multidimensional observed data. The question of ICA must find different solutions only by using the mutually statistical independence between source components and estimating the mixing matrix and source signals from receiving signals. For this reason, basic assumptions are needed to get a defined solution for ICA.

(1)Mutually statistical independence between signal components

As the core assumption for ICA, mutually statistical independence between signal components is a must for the estimating algorithm. On the condition that the assumption is satisfied, the ICA model is able to be established, which may explain why ICA can be widely applied in a variety of fields.

A set of random variable statistical independence is referred to the united probability density function (PDF) that can be decomposed into the multiplication of the marginal probability density function of each component. That is,

$$p(y_1, y_2, ...y_n) = p_1(y_1)p_2(y_2)...p_n(y_n) \quad (1)$$

Where, y_i represents the random variable, $p(y_1, y_2, ...y_n)$ the joint probability density function (PDF), $p_i(y_i)$ the marginal probability density function. Considering the unknown probability density function of random variables, it is difficult to measure the independence from the probability density. In this view, the random variable moment is adopted. Suppose random variable x and y satisfying the following formula when p and q are any integrate.

$$E\{x^p y^q\} - E\{x^p\}E\{y^q\} = 0 \quad (2)$$

(2) Signal components are non-gaussian or at most one Gaussian component is allowed

In view that the linear mixture of random variables are of gaussian distribution with zero high-order statistical value, ICA fails to achieve the blind separation between multiple stable gaussian source signals if there is no prior knowledge.

(3)Mixing matrix as the full column rank invertible matrix

The dimensions of mixing data are required to be bigger than or equal the number of independent components so that all components can be extracted.

In fact, the above-mentioned assumptions can be satisfied. The implementation of ICA generally include the following three steps:

Step 1:Whitening preprocessing

Whitening preprocessing includes the deduction of mean value and prewhitening. The observed data are first decentralized and then the observed vector is changed into zero mean value vector. The purpose of deducting mean value is to simplify the ICA algorithm by estimating the mixing matrix from the processed observed data before adding the mean value of source signals to the estimated signals. The whitening processing is to find a linear whitening matrix so that the

components of output signals after transformation are mutually independent. The common whitening methods is to adopt PCA using the eigenvalue decomposition (EVD) of covariance matrix of signals after deducting the mean value.

Step 2:Define objective function

Using the separated matrix as the dependent variablethe objective function represents the corresponding independence of each component for the output random vector. Two major requirements for objective function are:

(1)when variables are gaussian, the objective function's value is zero

(2)The stronger non-gausianness means the bigger absolute value of the objective function. When the objective function reaches its maximum, the component is independent.

Step3:Select a learning algorithm to optimize the objective function

After the objective function is defined, a learning algorithm is need o get the maximum or minimum value of the function through iteration.

Such statistical attributes as the consistency and robustness depend on the selection of objective function while the convergence and stability rely on the choice of learning algorithm. Some frequently used ICA algorithms include H-J, the minimum mutual information, information maximizing, maximum likelihood estimating and fixed points.

At present, the mainstream of ICA is fast Iteration algorithm (FastICA) based on fixed points. The basic algorithm is as follows:

Step1: Centre and whiten the data to get x according to following formula

$$x \leftarrow x - E\{x\} \tag{3}$$

$$x \leftarrow ED^{-1/2}E^T x \tag{4}$$

where,$E\{xx^T\} = EDE^T$, E is the eigenvector of covariance matrix $E\{xx^T\}$ and D is the eigenvalue matrix.

Step 2: Select initial weight vector w.

Step 3: Calculate w^+ according to following formula

$$w^+ \leftarrow E\{xg(w^T x)\} - E\{g^{'}(w^T x)\}w \tag{5}$$

$$w^+ \leftarrow \frac{w^+}{||w^+||} \tag{6}$$

where, function g derivates from the function G in the general contrast function.

Step 4: If not converged, go back to 3.

The workflow is illustrated in Fig.5.

FastICA is essentially a neural network approach of minimizing component's mutual information. It

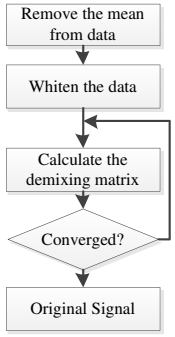

Figure 5: fastICA algorithm flowchar

uses the maximum entropy principle to approximate the negative entropy to achieve the optimization through an appropriate nonlinear function g. Its major merits are

(1) The algorithm is convenient with no need to select step size parameters.

(2) Faster convergence. Under the assumption of ICA data model, the convergence of FastICA is at least quadratic, by far faster than the common ICA linear convergence.

(3) Fewer computation. Using FastICA, work can be done only by estimating independent components one by one with no need to estimate all independent components at one time.

(4) FastICA can be optimized by selecting appropriate nonlinear function g and the algorithm of minimum variance can be achieved.

(5) In the case of FastICA, any independent components of non-Gaussian distribution can be found by using a nonlinear function g.But in the case of other algorithms, nonlinearity is a must on the condition that an estimation of probability density function is required before the nonlinear selection.

4 Proposed Scheme

As mentioned before, contourlet transform is an ideal watermark embedding domain in that it can capture geometrical structure of images in many directions even in multiscale space and describe images more sparsely. In addition, from the perspective of image processing, watermark embedding can be regarded as a process mixing the mutually independent host image signals with watermark signals while watermark extracting is a process of separating signals. In this sense, ICA is applicable in watermarking schemes. This paper thus designs watermark embedding and extracting algorithms combining ICA and contourlet transform. To boost the embedding capacity and improve the imperceptibility, the scaling factor in this paper is created as a matrix that varies with the host

image, differing from the traditional constant mentioned in the majority of traditional literatures. The proposed watermark scheme embraces three parts: the watermark embedding in Section 4.1; the extracting in Section 4.2 and the computation of scaling factor in Section 5.

4.1 Watermark Embedding

The embedding algorithm includes the following major eight steps:

Step 1: Read the host image and perform contourlet transform to get low frequency subimage I_0.

Step 2: Conduct a priority scaling of rows over I_0 into the one-dimension vector s_1.

$$s_1 = C_{2\to1}(I_0) \tag{7}$$

Step 3: Calculate the watermark scaling factor Λ obtained from the self-adaptive calculation according to the texture and edge of the host image. Details can be found in Section 5.

Step 4: Read the primitive watermark W_0 and perform the preprocessing

$$W = \Lambda * (W_0 - u) \tag{8}$$

where, $*$ represents Schur product.

$$u = \frac{1}{MN}\sum_{i=1}^{M}\sum_{j=1}^{N} W_0(i,j) \tag{9}$$

Step 5: The processed watermark W is converted into one-dimension vector s_2 according to the row priority principle.

Step 6: Embed watermark and regard x_2 as the key image.

$$\begin{pmatrix} x_1 \\ x_2 \end{pmatrix} = A \begin{pmatrix} s_1 \\ s_2 \end{pmatrix} \tag{10}$$

where, A is the random mixing matrix.

Step 7: Process x_1 into two dimension to get I_0^*

$$I_0^* = C_{1\to2}(x_1) \tag{11}$$

Step 8:Perform the inverse contourlet transform to get the embedded image I_w^*.

The process is illustrated in Fig.6.

4.2 Watermark Extracting

As the inversion of watermark embedding, the extracting is as follows:

Step 1: Perform contourlet transform over the embedded image I_w^* to get low frequency subimage I_0^*.

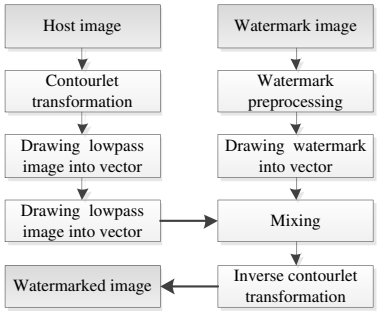

Figure 6: Watermark embedding

Step 2: Process I_0^* into one dimension to get x_1^*

$$x_1^* = C_{2\to1}(I_0^*) \tag{12}$$

Step 3: Use fastICA in Section 3 to get demixing matrix B.

Step 4: Calculate primitive signals s_1^* and s_2^*

$$\begin{pmatrix} s_1^* \\ s_2^* \end{pmatrix} = B \begin{pmatrix} x_1^* \\ x_2 \end{pmatrix} \tag{13}$$

Step 5: Process s_2^* into two dimension to get W^*

$$W^* = C_{1\to2}(s_2^*) \tag{14}$$

Step 6: Calculate to get the final watermarking image

$$W_0^* = \frac{W^*}{\Lambda} + u \tag{15}$$

where, u is the mean value of original watermark.

The process is displayed in Fig.7.

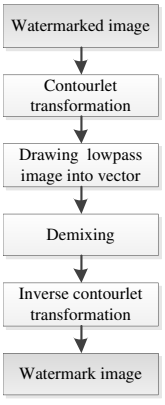

Figure 7: Watermark Extracting

5 Scaling Factor Calculation

Scaling factor as the key to balancing the robustness and imperceptibility in image watermarking is traditionally a constant with the same embedment strength

in different host images. As the ultimate receptor of image information, human's visual sense has redundancy and is insensible to a certain noise. Accordingly, for most watermark applications, watermarks of different embedment are embedded in different regions to boost the robustness.There are some human visual maskings closely involved in watermark embedding.

(1) Luminance characteristics. Human's visual sense is not much sensible to noise in highly bright regions, so that the higher brightness is accompanied by the more embedded information.

(2) Texture characteristics. The complexity of image background texture is responsible for the insensibility of human's visual sense to disturbing signals and more embedding information.

(3) Frequency characteristics. Studies indicate that human's visual sense is not so sensible to high-frequency content when images are transformed from the spatial domain to the frequency domain. Low-frequency components are in the smooth regions of image in spatial domain.

(4) Directional characteristics. Human's visual sense has a directional selection when observing image and is more sensible to changes in the diagonal direction than those in horizontal and vertical directions.

Combining the luminance and texture of the host image with the noise visibility function, this paper gives a dynamic computation of scaling factor shown in Fig.8. The following is the computation of scaling

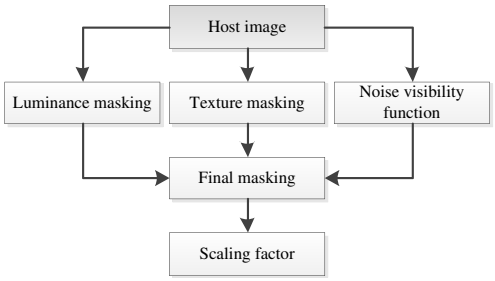

Figure 8: Scaling factor computing

factor in detail through HVS.

$$\Lambda = \alpha(1-(1-M_L(I))\times M_T(I)\times(1-NVF(I))) \tag{16}$$

where, α represents the embedment strength of 0.2 in the experiment,M_L the luminance masking, M_T the texture masking, NVF the noise visibility function.

(1) Calculate M_L

M_L is computed according to following formula in reference [14]

$$M_L(x,y) = \max\{f_1(bg(x,y),mg(x,y)), f_2(bg(x,y))\} \tag{17}$$

where, f_1, f_2, mg, bg are the spatial masking function, the visibility function, the maximum weighted average of luminance differences and the background luminance respectively. f_1, f_2, mg are computed by formula (18)-(23)

$$f_1(bg(x,y),mg(x,y)) = mg(x,y)\alpha(bg(x,y)) + \beta(bg(x,y)) \tag{18}$$

$$f_2(bg(x,y)) = \begin{cases} 17\left(1-\left(\frac{bg(x,y)}{127}\right)^{0.5}\right)+3, bg \le 127 \\ \frac{3}{128}(bg(x,y)-127)+3, bg > 127 \end{cases} \tag{19}$$

$$\alpha(bg(x,y)) = 0.0001bg(x,y) + 0.115 \tag{20}$$

$$\beta(bg(x,y)) = \frac{1}{2} - 0.01bg(x,y) \tag{21}$$

$$mg(x,y) = \max\{|grad_k(x,y)|\}, k = 1,2,3,4 \tag{22}$$

$$grad_k(x,y) = \frac{1}{16}\sum_{i=1}^{5}\sum_{j=1}^{5} p(x-3+i, y-3+j)G_k(i,j) \tag{23}$$

where, $p(x,y)$ is the pixel value at the position . The size of image block is $H \times W$. The values of $G_k(k=1,2,3,4)$ in formula (23) are shown in Fig.9 (a),(b) and Fig.10 (a),(b) [15]. x, y satisfy $0 \le x < H, 0 \le y < W$.$bg(x,y)$ is calculated by

$$bg(x,y) = \frac{1}{32}\sum_{i=1}^{5}\sum_{j=1}^{5} p(x-3+i, y-3+j)B(i,j) \tag{24}$$

where, the value of B is defined in Fig.10 (c) [15] and x, y satisfy $0 \le x < H, 0 \le y < W$.

0	0	0	0	0
1	3	8	3	1
0	0	0	0	0
-1	-3	-8	-3	-1
0	0	0	0	0

(a)G_1

0	0	1	0	0
0	8	3	0	0
1	3	0	-3	-1
0	0	-3	-8	0
0	0	-1	0	0

(b)G_2

Figure 9: The value of G_1, G_2

0	0	1	0	0
0	0	3	8	0
-1	-3	0	3	1
0	-8	-3	0	0
0	0	-1	0	0

(a)G_3

0	1	0	-1	0
0	3	0	-3	0
0	8	0	-8	1
0	3	0	-3	0
0	1	0	-1	0

(b)G_4

1	1	1	1	1
1	2	2	2	1
1	2	0	2	1
1	2	2	2	1
1	1	1	1	1

(c)B

Figure 10: The value of G_3, G_4 and B

(2) Calculate M_T

M_T is calculated according to formula (25) in reference [14]

$$M_T = |p(x,y) - \bar{p}(x,y)| \tag{25}$$

$$\bar{p}(x,y) = \frac{1}{(2L+1)^2} \sum_{i=-L}^{L} \sum_{j=-L}^{L} p(x+i, y+j) \tag{26}$$

where, $\bar{p}(x,y)$ is the mean value of the local domain $(2L+1) \times (2L+1)$. (3) Calculate NVF

NVF is calculated according to the formula(27) in reference [16]

$$NVF(x,y) = \frac{1}{1+\sigma^2(x,y)} \tag{27}$$

where, $\sigma^2(x,y)$ is the local variance of the window image in the scale of $(2L+1) \times (2L+1)$ with the pixel (x,y) at its core. The local variance is computed by

$$\sigma^2(x,y) = \frac{\sum_{i=-L}^{L} \sum_{j=-L}^{L} (p(x+i, y+j) - \bar{p}(x,y))^2}{(2L+1)^2} \tag{28}$$

The scaling factor of the host images Lena, Cameraman, Airplane, Lake, Peppers, Couple is manifested in Fig.11 (for the sake of convenience, the figure only presents the value of Λ/α). Fig.10 shows that brighter regions have bigger scaling factor and the embedding regions complying with HVS are focused in the edge and texture.

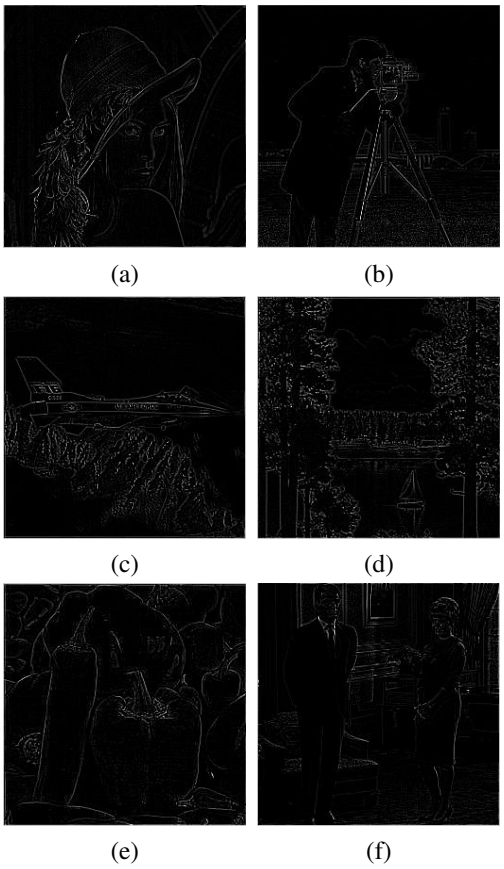

Figure 11: Scaling factor : (a)Lena,(b) Cameraman ,(c) Airplane,(d) Lake,(e)Peppers and (f) Couple

6 Computer Simulation Results

6.1 Experimental setup

This experiment employs 512×512 Lena, Cameraman, Airplane, Lake, Peppers, Couple as the primitive host images, the 64×64 gray image as the watermark image as shown in Fig.12. Contourlet transform uses "9/7"LP filter since the filter has linear phase and approximate orthogonality that are more adaptive to image signal processing. DFB for controulet transform adopts "pkva" as the directional filter with the embedment strength of 0.2. Considering the length limitations, this paper only presents the result of the host image Lena.

PSNR [9] is here adopted to calculate the imperceptibility

$$PSNR = 10\log_{10}\left(\frac{255^2}{MSE}\right) \tag{29}$$

$$MSE = \frac{1}{MN} \sum_{i=1}^{M} \sum_{j=1}^{N} (I(i,j) - I_w(i,j))^2 \tag{30}$$

When watermark is embedded into the host image Lena, Cameraman, Airplane, Lake, Peppers and Couple, their PSNR are 37.2044, 37.0951, 36.9896, 37.1322, 37.1126 and 37.7245 respectively, which satisfies the imperceptibility of watermark as demonstrated in Table 1. To test the robustness, NCC [12] is

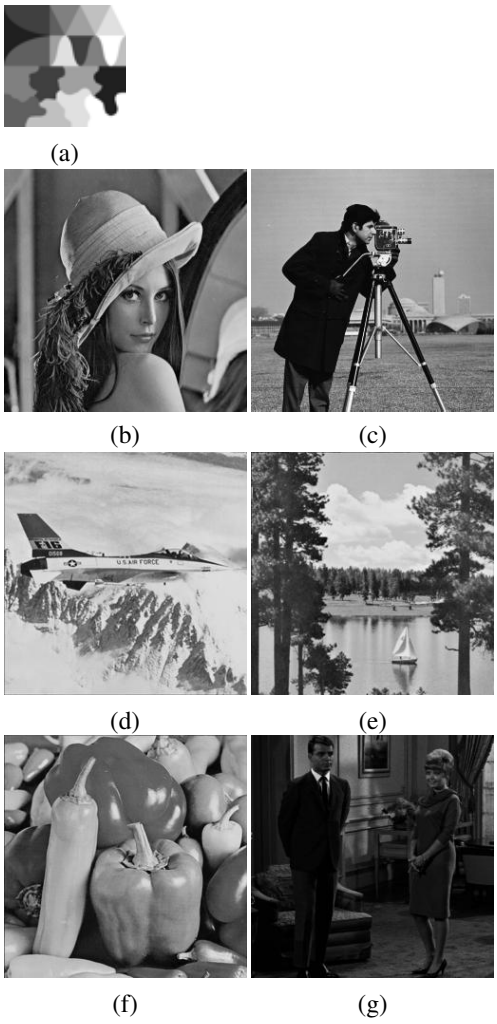

(a)

(b) (c)

(d) (e)

(f) (g)

Figure 12: Cover image and watermark: (a) watermark image (b) Lena,(c) Cameraman ,(d) Airplane,(e) Lake,(f) Peppers and (g) Couple

used.

$$NCC(W_0^*, W_0) = \frac{\sum_{i=1}^{P}\sum_{j=1}^{Q} W_0^*(i,j)W_0(i,j)}{\sqrt{\sum_{i=1}^{P}\sum_{j=1}^{Q} W_0^*(i,j)^2}\sqrt{\sum_{i=1}^{P}\sum_{j=1}^{Q} W_0(i,j)^2}} \quad (31)$$

6.2 Robustness Test

To test the robustness, the watermarked image has experienced common attacks including noising, filtering and cropping that are elaborated below.

Experiment 1(Noise attack): in the experiment, the watermarked image first experienced two noise attacks, one is the Salt & Pepper noise of density 0.005 and the other is Gaussian white noise with zero mean and variance 0.001. Fig.12 (b1) (b2) represent the two watermarked images when attacked by the abovementioned noises. The NCC values between the watermarked image and the primitive image are 0.8690 and 0.9036 respectively. Fig.13 shows the algorithm is successful in extracting the watermark image

Table 1: The results of imperceptibility

Host image	Lena	Cameraman	Airplane
PSNR	37.2044	37.0951	36.9896
Host image	Lake	Peppers	Couple
PSNR	37.1322	37.1126	37.7245

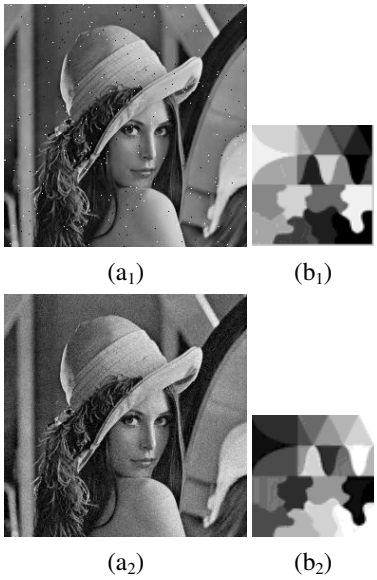

(a_1) (b_1)

(a_2) (b_2)

Figure 13: Result of experiment 1:(a1) Watermarked image under Salt & Pepper noise attack,(b1) Extracted watermark image,(a2) Watermarked image under Gaussian noise attack,(b2) Extracted watermark image

Experiment 2(JPEG compression attack): the watermarked image is conducted a compression with quality factor of 70% before extracting the watermark. The NCC value between the extracted image and the primitive image is 0. 8858. Fig.14 manifests that the extracted image is sound and clear.

Experiment 3(histogram equalization): the watermarked image is performed a histogram equalization as shown in Fig.15. The NCC value is 0.9036. Fig.14 (b) shows that ICA has facilitated the extraction of watermarking image and the Scheme enjoys good ability of resisting histogram equalization attack

Experiment 4(filtering attack): the watermarked image is performed the median filtering attack as shown

(a) (b)

Figure 14: Result of experiment 2: (a) Watermarked image under JPEG compression attack, (b) Extracted watermark image

(a) (b)

Figure 15: Result of experiment 3: (a) Watermarked image under histogram equalization attack,(b) Extracted watermark image

in Fig.16. The NCC value is 0.9034. The Fig.15 (b) demonstrates that it is good to extract the watermark image.

(a) (b)

Figure 16: Result of experiment 4: (a) Watermarked image under filtering attack,(b) Extracted watermark image

Experiment 5(cropping attack): the watermarked image is performed a 25% left bottom cropping. The NCC value is 0.8602.Fig.17 (b) shows that this algorithm is successful in extracting the watermark.

Experiment 6 (mirroring): The last experiment is to conduct a diagonal mirroring attack over the watermarked image. The NCC value is 0.8696.

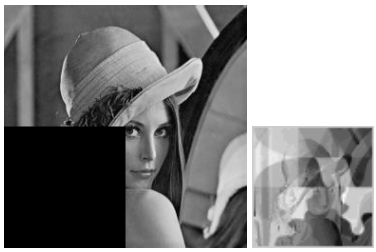

(a) (b)

Figure 17: Result of experiment 5: (a) Watermarked image under cropping attack,(b) Extracted watermark image

(a) (b)

Figure 18: Result of experiment 6: (a) Watermarked image under mirroring attack,(b) Extracted watermark image

7 Conclusion

A robust watermarking scheme in contourlet domain is designed in this paper based on ICA. The experiment has demonstrated that the scheme not only well satisfies imperceptibility but resisting frequent attacks such as Peppers & Salt noise, compression, filtering and mirroring with good robustness.

Acknowledgements: The paper is financed by State Natural Science Foundation (No.61163055, 60803157, 90812001, 61170271), National 242 program, the scientific foundation of the Ministry of Education (No.11YJCZH152), NSF of Zhejiang province(No.LQ12F02007) and the ECJTU (No.09XX03) research program.

References:

[1] M. Ouhsain, A. B. Hamza, Image watermarking scheme using nonnegative matrix factorization, *Expert Systems with Applications*, vol.36, no.2, 2009,pp. 2123-2129.

[2] Kwitt, R. Meerwald, P. Uhl, Lightweight detection of additive watermarking in the DWT-domain, *IEEE Trans. on Image Processing*, vol.20. no.2, 2011, pp.474-484.

[3] W. C. Chu, DCT based image watermarking using subsampling, *IEEE Trans on Multimedia*, vol.5, no.1, 2003, pp.34-38.

[4] V. Solachidis, I. Pitas, Circularly symmetric watermark embedding in 2-D DFT domain, *In Proceedings of the IEEE International Conference on Acoustics, Speech and Signal Processing*, vol. 6, 1999, pp.3469-3472.

[5] M. N. Do, M. Vetterli, The contourlet transform:An efficient directional multiresolution image representation,*IEEE Trans. on Image Processing*, vol.14, no.12, 2005, pp.2091-2106.

[6] M. Jayalakshmi, S. N. Merchant, U. B. Desai, Blind watermarking in contourlet domain with improved detection. *Proceeding of Intelligent Information Hiding and Multimedia Signal Processing*, 2006, pp.449-452.

[7] B. C. Mohan, S. S. Kumar, Robust digital watermarking scheme using contourlet transform,*International Journal of Computer Science and Network Security*, vol.8, no.2, 2008, pp.43-51.

[8] Farhad Rahimi, Hossein Rabani, A visually imperceptible and robust image watermarking scheme in contourlet domain, *IEEE International Conference on Signal Processing*, 2010, pp.1817-1820.

[9] T. V. Nguyen, J. C. Patra, A simple ICA-based digital image watermarking scheme, *Digital Signal Processing*,vol.18, no.5, 2008, pp.762-776.

[10] S. J. Ren, X. Su, H. S. Yu, H. J. Niu, Blind watermarking based on fastICA and DWT,*Proceedings of the 2009 International Workshop on Information Security and Application*, 2009, pp.256-259.

[11] A. Umaamaheshvari, K. Thanushkodi, Digital image watermarking based on ICA and ridgelet transform,*International Journal of Computer Science and Network Security*, vol.11, no.4,2011, pp.14-17.

[12] S. G Oskooei, M. Dadgostar, G. R. Rad, E. Fatemizadeh, Adaptive watermarking scheme based on ICA and RDWT, *3rd International Conference on Crime Detection and Prevention*, 2009, pp.1-4.

[13] P. Mangaiyarkarasi, S. Arulselvi,Robust color image watermarking technique based on DWT and ICA,*International Journal of Computer Applications*,vol.44, no.23, 2012, pp.6-12.

[14] H. Qi, D. Zheng, J. Zhao, Human visual system based adaptive digital image watermarking, *Signal Processing*, vol. 88, 2008, pp.174-188.

[15] Z. Wang, Q. Li, Information content weighting for perceptual image quality assessment, *IEEE Trans. on Image Processing*, vol.20, no.5, 2011, pp.1185-1198.

[16] F. Deguillaume, S. Voloshynovskiy, T. Pun, Secure hybrid robust watermarking resistant against tampering and copy-attack, *Signal Processing*, vol. 83, no.10, 2003, pp.2133-2170.